



Effect of cellulase on antioxidant activity and flavor of *Rosa roxburghii* Tratt

Guilan Jiang, Binbin Li, Zhuhong Ding^{*}, Jingyi Zhu, Silin Li

School of Liquor and Food Engineering, Guizhou University, Guiyang 550025, China

ARTICLE INFO

Keywords:

Cellulase
Rosa roxburghii Tratt
 Antioxidant activity
 HS-GC-IMS
 Electronic nose
 Electronic tongue
 Flavor

Chemical compounds studied in this article:

Butanal (PubChem CID: 261)
 (E)-Hept-2-enal (PubChem CID: 5283316)
 2-Methylpropanal (PubChem CID: 6561)
 2,3-Butanediol (PubChem CID: 262)
 1-Butanol (PubChem CID: 263)
 Methyl acetate (PubChem CID: 6584)
 Tert-butylmethylether (PubChem CID: 15413)
 2-Ethylfuran (PubChem CID: 18554)
 Pentanal (PubChem CID: 8063)
 2-Propanethiol (PubChem CID: 6364)

ABSTRACT

Cellulase can increase the soluble dietary fiber (SDF) content in *Rosa roxburghii* Tratt (RRT), but the effects on polyphenol content, bioactivity, and flavor are unknown. This study analyzed the changes in SDF content, total phenolic content, antioxidant activity and flavor before and after cellulase treatment. Cellulase treatment increased the SDF and total phenolic content of RRT by 13 % ($P < 0.05$) and 25.68 % ($P < 0.05$), respectively, and increased the antioxidant activity. HS-GC-IMS identified a total of 42 volatile compounds present, and ROAV analysis revealed that the characteristic aroma compounds of RRT were mainly aldehydes, alcohols, and ethers. The electronic nose and tongue results were consistent with the HS-GC-IMS analysis, indicating the positive effect of cellulase on the quality of RRT. Cellulase treatment significantly improved the oxidative activity and flavor performance of RRT. These results of RRT, providing practical guidance for improving the flavor and product quality.

1. Introduction

Rosa roxburghii Tratt (RRT) is a fruit from the Rosaceae family that is abundant in vitamins, dietary fiber, flavonoids, phenolic acids, and other active components. It has antioxidant, immune system regulatory, and anticancer properties (Wang et al., 2023). Due to its unique features, it has become a popular medicinal and dietary fruit in the southwest of China. Dietary fibers in foods are classified as either soluble dietary fiber (SDF) or insoluble dietary fiber (IDF). SDF has a wider range of functional activities than IDF, including hypoglycemic, weight loss, and inflammation reduction activities (Chawla & Patil, 2010). The RRT had a total dietary fiber content of 79.84 ± 0.90 g/100 g (dry weight), comprising of 6.83 ± 0.32 g/100 g of SDF and 73.05 ± 1.19 g/100 g of IDF, with IDF content making up approximately 91.5 % of the total dietary fiber (Wang, Shen, Li, & Chen, 2020). Therefore, its potential health benefits may be enhanced by increasing the amount of SDF in

RRT as a percentage of total dietary fiber (Liu, Ao, Zheng, Liang, & Ren, 2022).

Cellulase acts on the β -1,4-glucosidic bond and is a multicomponent enzyme with multiple action sites (Zhang, Cao, Bi, & Li, 2022). The enzymatic method has several advantages over chemical and physical methods, including low addition, low energy consumption, low pollution levels, and high safety (de Souza & Kawaguti, 2021). Many studies have confirmed the improvement of juice viscosity, juice yield, and juice turbidity by the use of cellulolytic enzymes (Ozyilmaz & Gunay, 2023). Studies have shown that cellulolytic enzymes can hydrolyze cellulose and hemicellulose components to increase SDF content (Ma et al., 2022). Additionally, it has been shown that cellulolytic enzymes can be used to promote the release of antioxidant compounds from fruits and vegetables, such as applications that promote the extraction of total polyphenols and increase antioxidant activity in passion fruit (Wang et al., 2021), and structural changes in the polysaccharides of yam and

^{*} Corresponding author.

E-mail address: gzdxzdh@163.com (Z. Ding).

<https://doi.org/10.1016/j.fochx.2024.101148>

Received 11 September 2023; Received in revised form 24 December 2023; Accepted 16 January 2024

Available online 17 January 2024

2590-1575/© 2024 The Authors. Published by Elsevier Ltd. This is an open access article under the CC BY-NC-ND license (<http://creativecommons.org/licenses/by-nc-nd/4.0/>).

increased antioxidant activity (Liu et al., 2022). RRT has a high dietary fiber content and low SDF content, which negatively impacts its processing, utilization, and edible quality. Currently, cellulases are primarily used for extracting and modifying RRT's dietary fiber properties (Li, Li, Fu, Huang, & Chen, 2023; Wu et al., 2020). However, there has been little investigation or attention given to the effects of cellulose-degrading enzyme treatment technologies on RRT's functional components, activities, and especially flavor quality.

This study investigated the relationship between cellulase and changes in SDF content, total phenolic content, and antioxidant activity in RRT. In addition, the study analyzed the effect of cellulase on the flavor of RRT using GC-IMS, electronic tongue, and electronic nose technology. The study aimed to explore the role of cellulase in improving the functional activity and flavor of RRT, and to provide theoretical and technological guidance for the application of enzymes to achieve high-value utilization of Rosa roxburghii Tratt resources and related improvement of resource quality.

2. Materials and methods

2.1. Samples

Fresh and disease-free mature RRT (Guinong 5, Longli, Guizhou, China) were selected and destoned, then the pulp was deseeded and mixed with water at a ratio of 1:1, and the pH of the mixture was adjusted to 5.0 using food grade sodium hydroxide. To each kilogram of pulp, 2 g of cellulase (10,000 U/g, from *Aspergillus niger*, Shanghai Aladdin Reagent Co., Ltd.) was added, stirred thoroughly, and reacted in a water bath at 40 °C for 4 h, followed by cooling in an ice bath for 20 min to stop the reaction. The samples to which cellulase was added comprised the experimental group (labeled as EX), while the samples that remained untreated with the enzyme formed the control group (labeled as CO).

2.2. SDF

The SDF content was determined according to the method of the National Standard of the People's Republic of China (GB5009.88-2014).

2.3. Determination of antioxidant activity

DPPH, ABTS, and OH radical scavenging activities were assessed in accordance with the assay kit instructions from Shanghai Liquid Quality Assay Technology Co., Ltd.

2.4. Total phenols

The method of Group Standard of the People's Republic of China (T/GZCX020/2022) was used to determine the total phenol content.

2.5. HS-GC-IMS

The volatile compounds in the samples were analyzed using a Flavour Spec1H1-00053 GC-IMS coupler from G. A. S (Germany). The sample was injected into an automatic headspace injection unit with a 200 µL volume injection. The incubation period was 20 min at a temperature of 40 °C, with a needle temperature of 85 °C and an incubation speed of 500 rpm. The volatile compounds in the samples were analyzed using headspace-gas chromatography-ion mobility spectrometry (HS-GC-IMS). The GC conditions were as follows: E1 (drift gas N₂), 0–20 min, 150 mL/min. E2 (carrier gas N₂), 0–2 min, 2 mL/min; 2–10 min, 10 mL/min; 10–20 min, 100 mL/min (Li et al., 2023). Flavor compounds were characterized by comparing the RIs and drift times of standards from the NIST database and the GC-IMS Library.

2.6. ROAV

The relative odor activity value (ROAV) of each flavor compound was calculated according to the equation proposed by Bi (Bi et al., 2022):

$$ROAV_X = 100 \times (C\%_X / C\%_{\text{stan}}) \times (T_{\text{stan}} / T_X)$$

Where ROAV_X represents the relative odor activity value of the flavor compounds, C%_X represents the relative percentage content of the flavor compounds, and T_X represents the threshold value of the flavor compounds. Meanwhile, C%_{stan} and T_{stan} are the relative percentage content and threshold value, respectively, of the flavor compounds that contribute most to the overall flavor. The relative percentage content of the flavor compounds was calculated through peak area normalization.

2.7. Electronic nose

The electronic nose system (PEN3, AIRSENSE, Germany) was utilized to analyze the RRT. The system included 10 metal oxide gas sensors. A 10 g sample was weighed and placed in a glass vial (15 mL), and the headspace determination was performed after standing for 1 h at 25 °C. The assay time and washing time were 70 s and 60 s, respectively.

2.8. Electronic tongue

Thirty g of each sample were weighed and mixed with 120 mL of water, then mixed and crushed for 1 min. Sample were filtered and 35 mL were introduced into the electronic tongue (SA402B, AIRSENSE, Germany) and detected at room temperature. Before and after each test, the detection head was washed with distilled water for 180 s.

2.9. Data analysis and statistics

HS-GC-IMS (G. A. S, Germany) analysis software included LAV (Laboratory Analytical Viewer), GC × IMS Library Search, Reporter plug-in, and Gallery Plot plug-in. Radar plots of the e-nose and e-tongue were plotted with Origin 2021 (OriginLab, USA). SIMCA 14.1 (Umetrics, Umeå, Sweden) was used to determine differences between samples.

3. Results and discussion

3.1. Analysis of SDF, total phenolics and antioxidant activity

RRT contains range of functional active ingredients, and the enhancement of the utilization of these ingredients is needed for efficient and accessible use. Table 1 shows that cellulase hydrolysis of RRT increased SDF content by 13 % (P < 0.05) and total phenolic content by approximately 25.68 % (P < 0.05).

The ABTS radical scavenging capacity of RRT rose significantly from 27.07 % (CO) to 49.23 % (EX) (P < 0.05). The DPPH scavenging capacity also increased from 54.00 % (CO) to 71.18 % (EX) (P < 0.05), while the OH radical scavenging capacity increased from 75.74 % (CO) to 86.36 % (EX) (P < 0.05). These results indicate that all three radical scavenging capacities were higher in the EX after enzymatic treatment compared to the CO. The levels of antioxidant activity in the DPPH assay are predicated on the hydroxyl groups within the structure of phenolic compounds, while the scavenging activity of ABTS is predominantly influenced by the presence of hydroxyl and methoxy groups, such as in

Table 1
Results of RRT indicators under different treatments.

Group	Items				
	SDF(g/100 g)	Total phenolic (mg/g)	ABTS (%)	DPPH (%)	OH (%)
CO	11.15	20.37	49.23	71.18	86.36
EX	12.6	25.60	27.07	54.00	75.74

phenolic acid, hydroxybenzoic acid, and hydroxycinnamic acid (Platzer, Kiese, Herfellner, Schweiggert-Weisz, & Eisner, 2021). It has been demonstrated that an escalation in phenolic compounds results in a rise in antioxidant activity. The DPPH scavenging activity positively correlates with the presence of gallic acid content ($P < 0.01$), while the ABTS scavenging activity positively correlates with both gallic acid and rutin content ($P < 0.01$) (Zhao, Tang, Cai, Peng, Zhang, & Shan, 2023). From 4 % to 57 % of the phenolic compounds found in fruits and vegetables are strongly linked to dietary fiber through either covalent bonds, hydrophobic bonds, or hydrogen interactions (Huang et al., 2022). Štátná et al. have reported that caffeic acid, protocatechuic acid, gallic acid, ferulic acid, epigallocatechin and quercetin were the major contributors to the antioxidant activity of the insoluble bound fractions (Štátná, Mrázková, Sumczynski, Cindik, & Yalçin, 2019). Dansi Huang et al. also found that RRT pomace is rich in gallic acid, ferulic acid, ellagic acid, quercetin, and other phenolic substances (Huang et al., 2022). In summary, the enhanced antioxidant activity of EX may be a result of cellulase hydrolyzing the cellular structure of RRT and promoting the release of gallic acid and other phenolics from RRT.

3.2. HS-GC-IMS analysis

HS-GC-IMS detected RRT volatile organic compounds (VOCs) while generating a 3D topographic map, shown in Fig. 1(a), where the x, y, and z axes represent ion migration time, ion relative drift time, and peak intensity, respectively. The 3D topographic map displays the raw data for all compounds, enabling the identification of signal peak intensities and positions for each volatile flavor compound in the sample.

The 2D spectrum is shown in Fig. 1(b), where the background of the entire figure is blue, the red vertical line at the horizontal coordinate 1.0 is the reactive ion peak (RIP, normalized), and each point on either side of the RIP peak represents a volatile organic substance. The colors correspond to the substance concentration, with white indicating lower concentration, red indicating higher, and darker colors indicating even higher concentration. The concentration and type of VOCs in various samples can be determined visually from the top view. Signals typically appeared with retention times between 50–150 s and drift times between 1.0 and 1.5 s.

HS-GC-IMS successfully separated 52 volatile compound signal peaks, and a total of 42 volatile compounds were identified by comparing the RIs and drift times of the standards from the NIST database and the GC-IMS Library. Some compounds were labeled with D and M at the end, denoting dimers and monomers, respectively, of the same substance. Results are presented in Table 2 and consist of 9 aldehydes, 9 alcohols, 9 esters, 5 ketones, and 10 other species.

The 2D and 3D spectra depict the trend of flavor compounds in the samples, while fingerprinting highlights changes in the content of specific flavor compounds and facilitates observation of differences in the changes of flavor compounds among different samples. Each line in Fig. 1(c) represented all the signals of each volatile aroma compound in different samples, and each column represented all the signals in each sample, and the darker and lighter colors indicated the concentration of each aroma compound, and the brighter the color, the higher the concentration of that compound.

The samples were found to contain the aldehydes 2-methyl-2-propenal, hexanal, (E)-hept-2-enal, 3-methyl-2-butenal, 2-methylpropanal-D, 2-methylpropanal-M, butanal-D, butanal-M. Aldehydes are associated with fatty, green, paint, light, fruity and soybean odors. They have a low odor threshold and contribute greatly to the flavor of foods (Li, Al-Dalali, Wang, Xu, & Zhou, 2022). Butanal has some bad odors, sour or choking irritating odors. And compared with CO, the relative content of butanal-M in EX was reduced after cellulase hydrolysis. (E)-hept-2-enal had a green, leafy, fatty odor, 2-methylpropanal-M had a malty odor, and pentanal had an aromatic odor, and all of them increased in EX. The formation of higher aldehydes may be correlated with increased levels of unsaturated fatty acids in their corresponding samples (Fan et al., 2021).

Arshad et al. suggested that straight-chain aldehydes are mainly derived from oxidative degradation of saturated or unsaturated lipids (Arshad et al., 2018), and García noted that branched-chain aldehydes are mainly derived from amino acid deamination and decarboxylation (García et al., 1991). In this study, GC-IMS identified primarily straight-chain aldehydes as the main flavor compounds present in RRT, demonstrating that lipid oxidative degradation was the primary mechanism producing these compounds. Enzymatic treatment increased desirable volatile compounds and decreased undesirable flavor compounds in RRT.

Among the alcohols identified in the RRT, 2,3-butanediol has a buttery aroma. 1-butanol, 2-propanol-M, and ethanol have a fresh, fruity, and herbal alcohol aroma. *Tert*-butanol has a camphor-like aroma, 1-propanol has an alcoholic, candy, and pungent aroma, and 3-methyl-2-butanol has a sweet and honey-like aroma. Cellulase hydrolysis has been shown to increase the levels of 2,3-butanediol, 1-butanol. These alcohols act as a complement to the ester flavor, thereby increasing its intensity. They allow the flavor to be released slowly and persist longer, which is important to aroma and flavor in the product (Li et al., 2023).

Esters play a significant role in the development of RRT aromas due to their low threshold and association with floral and fruity aromas (Wang et al., 2023). Ethyl formate, propyl acetate, isopentyl formate, ethyl propanoate, ethyl acrylate, isopropyl acetate, butyl formate, methyl acetate-M, and methyl acetate-D were identified as the esters in this study. The CO had a high methyl acetate content, which decreased after enzymatic treatment. According to previous research, a reduction in the activity of lipoxygenase, a lipid oxidation pathway, may have an effect on the loss of methyl acetate in fruit pulp (Bai et al., 2011). Furthermore, phenolics have been shown to inhibit lipoxygenase (Lončarić et al., 2021). It is suggested that the decrease in methyl acetate content was due to the inhibition of lipoxygenase by the increase in phenolic content in RRT.

Five ketones were identified in RRT as 3-hydroxybutan-2-one, 2-hexanone, 1-penten-3-one, acetone, and acetoxyacetone. The ketones are generally considered to have fatty and burnt aromas and exhibit enhanced floral aromas with the extension of the carbon chain. Among other compound classes, *tert*-butylmethylether-D has a minty terpene aroma. 2-ethyl furan has a burnt aroma, pentanoic acid has a sweaty aroma, and propanoic acid has a pungent aroma. 2-Propanethiol-D has a raw onion aroma, and sulfur compounds are often considered key compounds despite their relatively low levels in foods (Yeo, Balagiannis, Koek, & Parker, 2022).

In summary, HS-GC-IMS identified volatile flavor compounds in both CO and EX. The content of compounds such as pentanal, (E)-hept-2-enal, 2-methylpropanal-M, 1-butanol and 2,3-Butanediol, which have pleasant odors, increased in EX compared to CO. Additionally, the content of undesirable flavor compounds such as *tert*-butylmethylether and butanal decreased in EX. These results suggest that cellulase reduced the undesirable flavors in RRT and improved its overall flavor quality.

3.3. Statistical analysis and differential screening

In order to more clearly illustrate the differences between the samples, we used the orthogonal partial least squares discriminant analysis (OPLS-DA) approach to investigate the sample differences. Specifically, we built an OPLS-DA model using the aroma profiles of EX and CO, as shown in Fig. 2(a). The model demonstrated strong goodness of fit ($R^2 = 0.975$, $R^2 = 1$), strong predictive ability ($Q^2 = 0.995$). The OPLS-DA model constructed was subjected to a 200 replacements test to assess its reliability. Fig. 2(b) displays the results, which reveal that the randomly generated R^2 and Q^2 are smaller than the original model. The Q^2 intercept is 0.306, indicating that the model has good reliability. The OPLS-DA model constructed was subjected to a 200 replacements test to check the reliability of the model. Fig. 2(b) displays the results, which

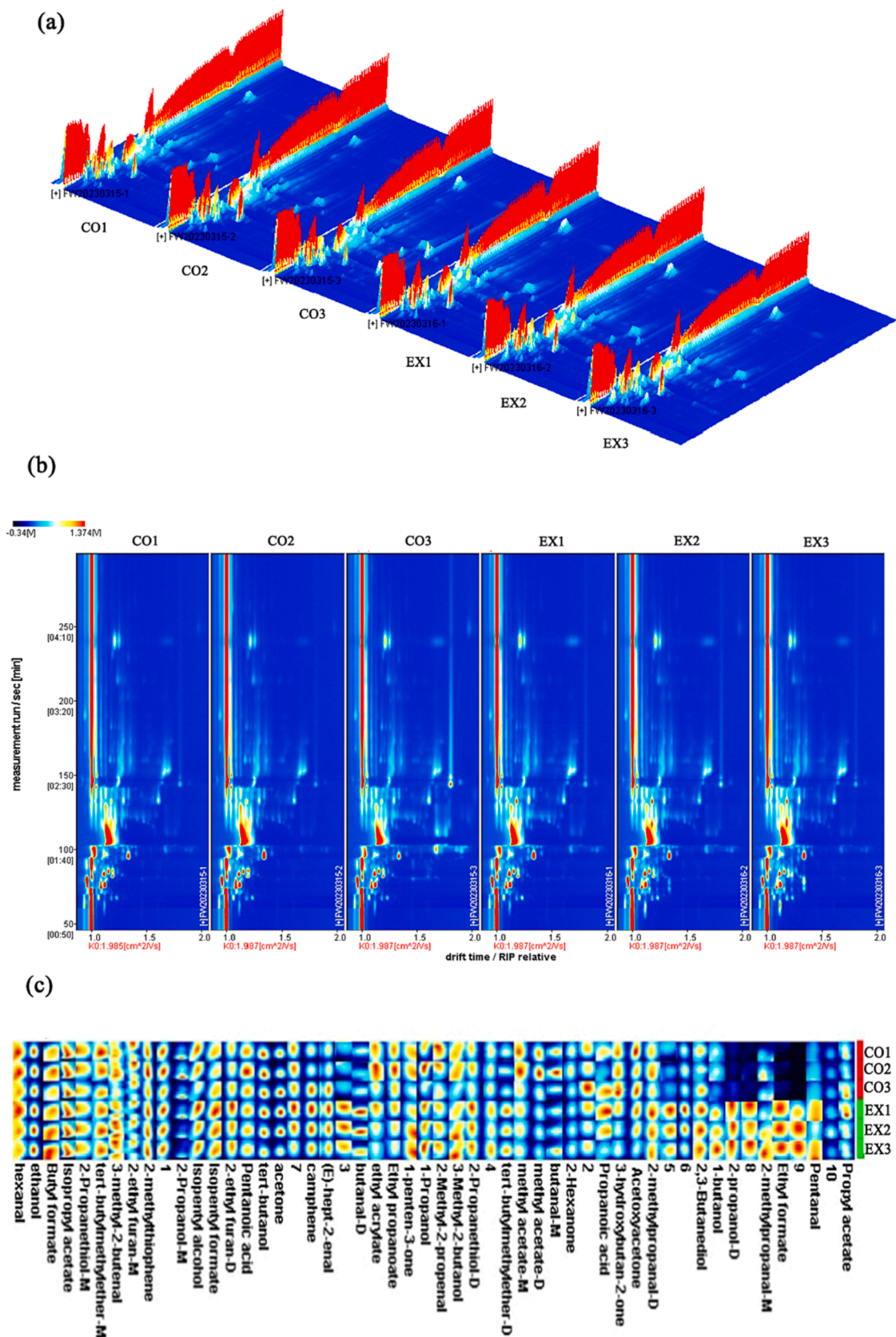


Fig. 1. 3D topographic map of VOCs in RRT generated by HS-GC-IMS (a), 2D map of VOCs in RRT generated by HS-GC-IMS (b), GC-IMS fingerprint of RRT (c).

Table 2
Volatile organic compounds in RRT.

No.	Compound	CAS	Formula	MW	RI	Rt [sec]
aldehyde						
1	(E)-hept-2-enal	C18829555	C7H12O	112.2	959.2	240.374
2	3-methyl-2-butenal	C107868	C5H8O	84.1	711.7	132.671
3	2-Methyl-2-propenal	C78853	C4H6O	70.1	580.9	99.107
4	hexanal	C66251	C6H12O	100.2	773	156.024
5	butanal-D	C123728	C4H8O	72.1	598.5	102.903
6	butanal-M	C123728	C4H8O	72.1	598.5	102.903
7	2-methylpropanal-D	C78842	C4H8O	72.1	558.4	94.448
8	pentanal	C110623	C5H10O	86.1	695.1	126.965
9	2-methylpropanal-M	C78842	C4H8O	72.1	538.9	90.582
alcohol						
10	3-methyl-2-butanol	C598754	C5H12O	88.1	654.8	116.076
11	<i>tert</i> -butanol	C75650	C4H10O	74.1	513.1	85.716
12	2-propanol-M	C67630	C3H8O	60.1	466.8	77.631
13	ethanol	C64175	C2H6O	46.1	462.9	76.984
14	1-propanol	C71238	C3H8O	60.1	557.6	94.286
15	2-propanol-D	C67630	C3H8O	60.1	480.2	79.895
16	2,3-butanediol	C513859	C4H10O2	90.1	782.1	159.78
17	isopentyl alcohol	C123513	C5H12O	88.1	746.3	145.385
18	1-butanol	C71363	C4H10O	74.1	664.2	118.447
esters						
19	propyl acetate	C109604	C5H10O2	102.1	673.1	120.73
20	isopentyl formate	C110452	C6H12O2	116.2	765.2	152.822
21	ethyl propanoate	C105373	C5H10O2	102.1	728.5	138.681
22	ethyl acrylate	C140885	C5H8O2	100.1	699.1	128.3
23	isopropyl acetate	C108214	C5H10O2	102.1	633.7	110.967
24	butyl formate	C592847	C5H10O2	102.1	734	140.71
25	methyl acetate-M	C79209	C3H6O2	74.1	523.6	87.656
26	methyl acetate-D	C79209	C3H6O2	74.1	514.9	86.039
27	ethyl formate	C109944	C3H6O2	74.1	497	82.805
ketones						
28	3-hydroxybutan-2-one	C513860	C4H8O2	88.1	727	138.141
29	2-hexanone	C591786	C6H12O	100.2	786.2	161.383
30	1-penten-3-one	C1629589	C5H8O	84.1	662.8	118.083
31	acetone	C67641	C3H6O	58.1	505.1	84.26
32	acetoxy acetone	C592201	C5H8O3	116.1	497.9	82.967
other						
33	pentanoic acid	C109524	C5H10O2	102.1	912.9	214.281
34	propanoic acid	C79094	C3H6O2	74.1	687.3	124.459
35	camphene	C79925	C10H16	136.2	959.2	240.374
36	2-ethyl furan-D	C3208160	C6H8O	96.1	713.4	133.249
37	2-ethyl furan-M	C3208160	C6H8O	96.1	713.7	133.364
38	2-methylthiophene	C554143	C5H6S	98.2	759.9	150.702
39	<i>tert</i> -butylmethylether-M	C1634044	C5H12O	88.1	574.9	97.83
40	<i>tert</i> -butylmethylether-D	C1634044	C5H12O	88.1	567	96.188
41	2-propanethiol-M	C75332	C3H8S	76.2	572	97.241
42	2-propanethiol-D	C75332	C3H8S	76.2	574.9	97.843

reveal that the randomly generated R^2 and Q^2 are smaller than the original model. The Q^2 intercept is 0.306, indicating that the model has good reliability. The OPLS-DA model constructed was subjected to a 200 replacements test to check the reliability of the model. Fig. 2(b) displays the results, which reveal that the randomly generated R^2 and Q^2 are smaller than the original model. The Q^2 intercept is 0.306, indicating that the model has good reliability. Therefore, the OPLS-DA model developed in this study is effective and suitable for analyzing inter-sample variation. Fig. 2(a) illustrates that EX and CO were distinguished into two groups with a larger distance between them and a smaller distance within each group. The results showed that EX and CO had larger between-group differences and their within-group differences were smaller. The collective outcomes displayed that cellulase treatment has a significant impact on RRT flavor adjustments.

Differences between samples were primarily determined by a small number of VOCs. Therefore, screening for distinct aroma compounds is useful for further analysis of the causes of differences between samples. The value of the variation weight parameter (VIP) is utilized to measure a variable's contribution to the variation of the samples, with larger VIP values indicating a more significant contribution. Usually, a compound with a $VIP > 1$ indicates its significance in contributing to sample differences. Based on the weight values ($VIP > 1$) of the established OPLS-

DA model (Fig. 2(c)), we screened 14 differential flavor compounds that included 2-propanol-M, camphene, isolate acetate, *tert*-butylmethylether-D, (E)-hept-2-enal, 1-butanol, methyl acetate-D, acetoxyacetone, 3-methyl-2-butenal, 2-methyl-2-propenal, acetone, ethyl acrylate, and two unidentified compounds. Among them, 2-propanol-M and camphene had the highest VIP values, indicating that these compounds were the primary contributors to the flavor differences between EX and CO.

3.4. ROAV analysis

To gain better insight into the distinct taste profiles of various samples, we utilized ROAV to assess the major contributors to aroma. $ROAV \geq 1$ indicate that the compound is likely to be a major contributor to the overall taste of the sample, while $0.1 \leq ROAV < 1$ indicates that the compound is a modifying flavor compound that alters the overall taste. The (E)-hept-2-enal, with a relative content of 2.5 % in the CO and 3.0 % in the EX, gives a distinct green, leafy, fatty flavor (Li et al., 2023). It has a significant influence on the overall flavor of RRT with a very low threshold (0.0005 mg/kg), which indicates that this compound has a significant influence on the overall flavor of RRT. Therefore, $ROAV_{stan}$ (E)-hept-2-enal was established as the standard at 100 to calculate the

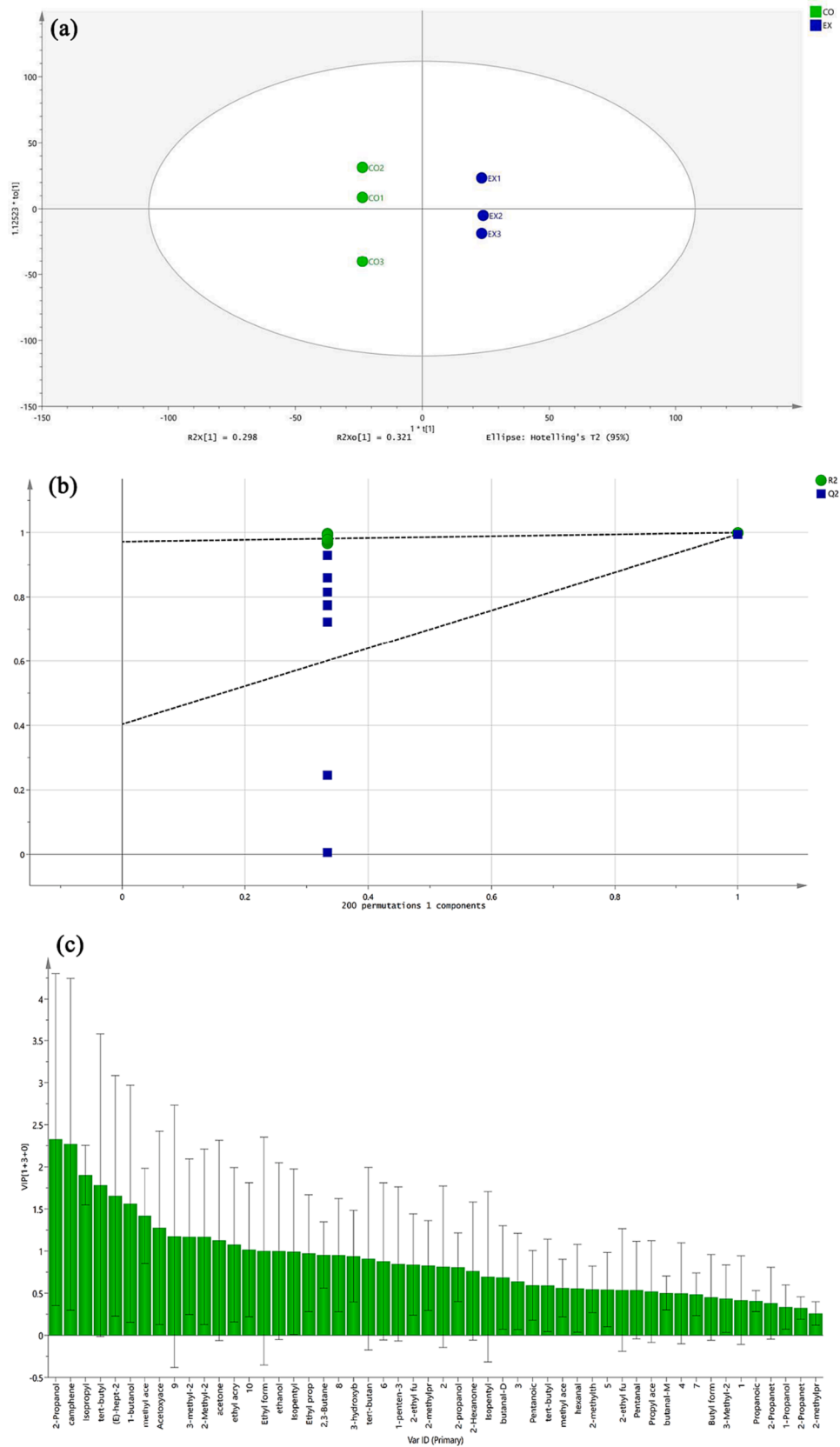


Fig. 2. Scatter plot presenting OPLS-DA scores for RRTs receiving different treatments (a), plot illustrating the outcomes of 200 substitution trials (b), and VIP score plot (c).

ROAV of other flavor compounds. Table 3 displays the thresholds, amounts, and flavor descriptions of the compounds with ROAV > 0.1. The characteristic flavor compounds of RRT were mainly aldehydes, alcohols, and ethers, and among them, seven were aldehydes, indicating that the flavor of RRT was mainly influenced by aldehydes. As shown in Table 3, there are 10 compounds with ROAV > 1, indicating that these 10 compounds are the characteristic odorants of RRT. Of them, *tert*-butylmethylether, which gives a minty, terpene-like odor, and ethyl acrylate, which gives a plastic-like odor, give an unpleasant sensation. Moreover, their ROAV values were higher in CO and lower in EX. In short, the majority of the distinctive aroma compounds in RRT were increased after it was treated with cellulase, which indicated that cellulase had a greater effect on the aroma of RRT and improved the aroma performance of it.

3.5. Electronic nose and electronic tongue analysis

The electronic nose sensor response was approximately stable after 66 s. Therefore, the electronic nose assay of the sample was analyzed using data from 66 to 68 s. The results are shown in Fig. 3(a). The radar plot indicates changes in response values for sensors W5S (for small molecule nitrogen oxides analogs), W2W (sensitive to aromatic constituents and organic sulfides), W2S (sensitive to ethanol), W1W (sensitive to sulfide), and W1S (sensitive to methane) after the sample was treated with cellulase. The response values of sensors W5S and W1S exhibited prominent changes. The results demonstrate a significant increase in nitrogen oxides and methane species in RRT post hydrolysis of cellulase. The obtained results were consistent with the changes in volatiles determined through HS-GC-IMS.

The electronic tongue, with its low sensory threshold, objectively reflects sample taste variability (Lu, Hu, Hu, Li, & Tian, 2022). Electronic tongue detection was utilized to differentiate taste characteristic variations between samples treated with differing treatment. After cellulase hydrolysis of the sample, detection results in Fig. 3(b) can be seen that the sour taste response value of the sample increased, the bitter taste is reduced, so that its palatability has been improved, while the rest of the taste sensor signal value did not change significantly. The release of some phenolics may have acidic properties (Du, Chen, Liu, Wang, & Kong, 2021). Polyphenols and tannins are the primary components contributing to the bitter and astringent taste of fresh fruits (Paissoni, Motta, Giacosa, Rolle, Gerbi, & Rio Segade, 2023; Zhao et al., 2023). The decrease in bitterness may be due to the formation of hydrolysis

products that mask the bitter and astringent properties (Lao, Zhang, Li, & Bhandari, 2020). The electronic tongue results corroborate the above results of changes in total phenolic content. In conclusion, it has been observed that the application of cellulase treatment resulted in an increase in the phenolic content of RRT and a desirable enhancement in its flavor presentation.

4. Conclusion

Analysis of changes in SDF, total phenol content, and antioxidant activity across different samples indicated that RRT hydrolyzed by cellulase significantly increased SDF, total phenol content, and antioxidant activity compared to samples without cellulase hydrolysis. The rise in antioxidant activity is thought to be the result of cellulase hydrolysis of RRT, leading to the release of phenolics from RRT. Cellulase hydrolysis reduced the levels of undesirable flavor compounds, including *tert*-butylmethylether and butanal, while increasing the amounts of aromatic compounds like Ethyl formate, Pentanal, 2,3-Butanediol, and other alcohols and esters in RRT. Analysis conducted with electronic nose and electronic tongue also indicated improved flavor quality of RRT, as cellulase treatment reduced bitterness. As a type of nutritious and healthy fruit resource with significant value for exploitation, this study can offer insights for the exploration of Rosa roxburghii Tratt resource functions and product development. Additionally, it presents a point of reference and guidance for the update and conversion of related technologies.

CRedit authorship contribution statement

Guilan Jiang: Investigation, Software, Formal analysis. **Zhuhong Ding**: Funding acquisition, Methodology, Writing – review & editing. **Jingyi Zhu**: Formal analysis, Data curation. **Silin Li**: Methodology.

Declaration of competing interest

The authors declare that they have no known competing financial interests or personal relationships that could have appeared to influence the work reported in this paper.

Table 3
Relative content of volatile compounds and their corresponding ROAV.

No.	Compounds	Odor threshold Value (mg/kg)	Relative content (%)		ROAV		Flavor description	References
			CO	EX	CO	EX		
1	(E)-hept-2 enal	0.0005	2.50	3.00	100	100	green, leaf, fat	(Li et al., 2023)
2	2-propanethiol-D	0.00005	0.20	0.22	78.08	73.26	raw onion	(Yeo et al., 2022)
3	2-methylpropanal-M	0.0007	0.25	0.39	7.27	9.19	malty	(Grimm & Steinhaus, 2019)
4	2-methyl-2-propenal	0.015	5.13	4.84	6.83	5.37		
5	<i>tert</i> -butylmethylether-D	0.015	4.29	4.78	5.70	5.30	minty	(Sun, Chen, Xiang, Hu, & Zhao, 2022)
6	ethyl propanoate	0.0049	1.34	1.11	5.45	3.78	nail polish-like	(Sun et al., 2018)
7	ethyl acrylate	0.018	1.81	1.52	2.01	1.41	plastic-like	(Sun et al., 2018)
8	<i>tert</i> -butylmethylether-M	0.015	1.00	0.91	1.34	1.01	minty	(Sun et al., 2022)
9	butanal-M	0.007	0.42	0.42	1.20	1.00	chocolate, malty	(Sun et al., 2022)
10	butanal-D	0.007	0.38	0.46	1.08	1.10	chocolate, malty	(Sun et al., 2022)
11	isopropyl acetate	0.9	30.93	30.01	0.69	0.56		
12	2-methylpropanal-D	0.007	0.23	0.22	0.67	0.53	malty, biting	(Stephan & Steinhart, 1999)
13	3-hydroxybutan-2-one	0.04	0.78	0.06	0.39	0.25	sweet, buttery, fatty, milky, creamy	(Sasanam et al., 2023)
14	camphene	0.45	4.06	5.01	0.18	0.19	green	(Ni, Jiang, Zhang, Huang, Li, & Chen, 2020)
15	hexanal	0.21	1.43	1.35	0.14	0.11	grass, tallow, fat	(Li et al., 2023)
16	isopentyl alcohol	0.25	1.47	1.53	0.12	0.10		

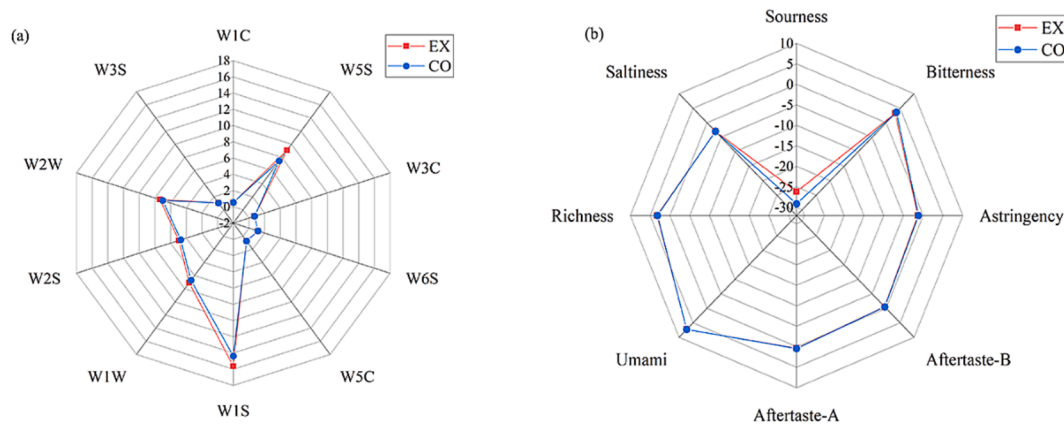


Fig. 3. Radar images of the electronic nose (a) and electronic tongue (b).

Data availability

Data will be made available on request.

Acknowledgment

This research was financially supported by the National Natural Science Foundation of China (Grant Nos. 32160523).

Appendix A. Supplementary data

Supplementary data to this article can be found online at <https://doi.org/10.1016/j.fochx.2024.101148>.

References

- Arshad, M. S., Sohaib, M., Ahmad, R. S., Nadeem, M. T., Imran, A., Arshad, M. U., & Amjad, Z. (2018). Ruminant meat flavor influenced by different factors with special reference to fatty acids. *Lipids in Health and Disease*, 17(1), 223. <https://doi.org/10.1186/s12944-018-0860-z>
- Bai, J., Baldwin, E. A., Imahori, Y., Kostenyuk, I., Burns, J., & Brecht, J. K. (2011). Chilling and heating may regulate C6 volatile aroma production by different mechanisms in tomato (*Solanum lycopersicum*) fruit. *Postharvest Biology and Technology*, 60(2), 111–120. <https://doi.org/10.1016/j.postharvbio.2010.12.002>
- Bi, J., Li, Y., Yang, Z., Lin, Z., Chen, F., Liu, S., & Li, C. (2022). Effect of different cooking times on the fat flavor compounds of pork belly. *Journal of Food Biochemistry*, 46(8). <https://doi.org/10.1111/jfbc.14184>
- Chawla, R., & Patil, G. R. (2010). Soluble dietary fiber. *Comprehensive Reviews in Food Science and Food Safety*, 9(2), 178–196. <https://doi.org/10.1111/j.1541-4337.2009.00099.x>
- de Souza, T. S. P., & Kawaguti, H. Y. (2021). Cellulases, Hemicellulases, and Pectinases: Applications in the Food and Beverage Industry. *Food and Bioprocess Technology*, 14(8), 1446–1477. <https://doi.org/10.1007/s11947-021-02678-z>
- Du, H., Chen, Q., Liu, Q., Wang, Y., & Kong, B. (2021). Evaluation of flavor characteristics of bacon smoked with different woodchips by HS-SPME-GC-MS combined with an electronic tongue and electronic nose. *Meat Science*, 182. <https://doi.org/10.1016/j.meatsci.2021.108626>
- Fan, X., Jiao, X., Liu, J., Jia, M., Blanchard, C., & Zhou, Z. (2021). Characterizing the volatile compounds of different sorghum cultivars by both GC-MS and HS-GC-IMS. *Food Research International*, 140, Article 109975. <https://doi.org/10.1016/j.foodres.2020.109975>
- García, C., Berdagüé, J. J., Antequera, T., López-Bote, C., Córdoba, J. J., & Ventanas, J. (1991). Volatile components of dry cured Iberian ham. *Food Chemistry*, 41(1), 23–32. [https://doi.org/10.1016/0308-8146\(91\)90128-B](https://doi.org/10.1016/0308-8146(91)90128-B)
- Grimm, J. E., & Steinhaus, M. (2019). Characterization of the major odor-active compounds in jackfruit pulp. *Journal of Agricultural and Food Chemistry*, 67(20), 5838–5846. <https://doi.org/10.1021/acs.jafc.9b01445>
- Huang, D., Li, C., Chen, Q., Xie, X., Fu, X., Chen, C., & Dong, H. (2022). Identification of polyphenols from *Rosa roxburghii* Tratt pomace and evaluation of in vitro and in vivo antioxidant activity. *Food Chemistry*, 377, Article 131922. <https://doi.org/10.1016/j.foodchem.2021.131922>
- Lao, Y., Zhang, M., Li, Z., & Bhandari, B. (2020). A novel combination of enzymatic hydrolysis and fermentation: Effects on the flavor and nutritional quality of fermented *Cordyceps militaris* beverage. *LWT*, 120. <https://doi.org/10.1016/j.lwt.2019.108934>
- Li, B., Zhang, T., Dai, Y., Jiang, G., Peng, Y., Wang, J., & Ding, Z. (2023). Effects of probiotics on antioxidant activity, flavor compounds and sensory evaluation of *Rosa roxburghii* Tratt. *LWT*, 179. <https://doi.org/10.1016/j.lwt.2023.114664>
- Li, C., Al-Dalali, S., Wang, Z., Xu, B., & Zhou, H. (2022). Investigation of volatile flavor compounds and characterization of aroma-active compounds of water-boiled salted duck using GC-MS-O, GC-IMS, and E-nose. *Food Chemistry*, 386. <https://doi.org/10.1016/j.foodchem.2022.132728>
- Li, M., Zhang, J., Li, L., Wang, S., Liu, Y., & Gao, M. (2023). Effect of enzymatic hydrolysis on volatile flavor compounds of *Monascus*-fermented tartary buckwheat based on headspace gas chromatography-ion mobility spectrometry. *Food Research International*, 163, Article 112180. <https://doi.org/10.1016/j.foodres.2022.112180>
- Li, P., Li, C., Fu, X., Huang, Q., & Chen, Q. (2023). Physicochemical, functional and biological properties of soluble dietary fibers obtained from *Rosa roxburghii* Tratt pomace using different extraction methods. *Process Biochemistry*, 128, 40–48. <https://doi.org/10.1016/j.procbio.2023.02.021>
- Liu, X., Gu, L., Zhang, G., Liu, H., Zhang, Y., & Zhang, K. (2022). Structural characterization and antioxidant activity of polysaccharides extracted from Chinese yam by a cellulase-assisted method. *Process Biochemistry*, 121, 178–187. <https://doi.org/10.1016/j.procbio.2022.06.023>
- Liu, Y., Ao, H.-P., Zheng, J.-X., Liang, Y.-X., & Ren, D.-F. (2022). Improved functional properties of dietary fiber from *Rosa roxburghii* Tratt residue by steam explosion. *Journal of Food Processing and Preservation*, 46(1), e16119.
- Lončarić, M., Strelec, I., Moslavac, T., Šubarić, D., Pavić, V., & Molnar, M. (2021). Lipoxigenase inhibition by plant extracts. *Biomolecules*, 11.
- Lu, L., Hu, Z., Hu, X., Li, D., & Tian, S. (2022). Electronic tongue and electronic nose for food quality and safety. *Food Research International*, 162, Article 112214. <https://doi.org/10.1016/j.foodres.2022.112214>
- Ma, Q., Ma, Z., Wang, W., Mu, J., Liu, Y., Wang, J., & Sun, J. (2022). The effects of enzymatic modification on the functional ingredient - Dietary fiber extracted from potato residue. *LWT*, 153. <https://doi.org/10.1016/j.lwt.2021.112511>
- Ni, H., Jiang, Q., Zhang, T., Huang, G., Li, L., & Chen, F. (2020). Characterization of the aroma of an instant white tea dried by freeze drying. *Molecules*, 25.
- Ozyilmaz, G., & Gunay, E. (2023). Clarification of apple, grape and pear juices by co-immobilized amylase, pectinase and cellulase. *Food Chemistry*, 398, Article 133900. <https://doi.org/10.1016/j.foodchem.2022.133900>
- Paissoni, M. A., Motta, G., Giacosa, S., Rolle, L., Gerbi, V., & Rio Segade, S. (2023). Mouthfeel subqualities in wines: A current insight on sensory descriptors and physical-chemical markers. *Comprehensive Reviews in Food Science and Food Safety*. <https://doi.org/10.1111/1541-4337.13184>
- Platzer, M., Kiese, S., Herfellner, T., Schweiggert-Weisz, U., & Eisner, P. (2021). How does the phenol structure influence the results of the folin-ciocalteu assay? *Antioxidants*, 10.
- Sasanam, S., Thumthanaruk, B., Wijuntamook, S., Rattananupap, V., Vatanyoopaisarn, S., Puttanlek, C., & Rungsardthong, V. (2023). Extrusion of process flavorings from methionine and dextrose using modified starch as a carrier. *PLoS One*, 18(2), e0269857.
- Štaštná, K., Mrázková, M., Sumczynski, D., Cindik, B., & Yalçın, E. (2019). The nutritional value of non-traditional gluten-free flakes and their antioxidant activity. *Antioxidants*, 8(11), 565. <https://www.mdpi.com/2076-3921/8/11/565>
- Stephan, A., & Steinhart, H. (1999). Quantification and sensory studies of character impact odorants of different soybean lecithins. *Journal of Agricultural and Food Chemistry*, 47(10), 4357–4364. <https://doi.org/10.1021/jf990105p>
- Sun, H., Chen, X., Xiang, Y., Hu, Q., & Zhao, L. (2022). Fermentation characteristics and flavor properties of *Herichium erinaceus* and *Tremella fuciformis* fermented beverage. *Food Bioscience*, 50. <https://doi.org/10.1016/j.fbio.2022.102017>
- Sun, J., Li, Q., Luo, S., Zhang, J., Huang, M., Chen, F., & Li, H. (2018). Characterization of key aroma compounds in Meilanchun sesame flavor style baijiu by application of aroma extract dilution analysis, quantitative measurements, aroma recombination, and omission/addition experiments. *Rsc Advances*, 8(42), 23757–23767. <https://doi.org/10.1039/c8ra02727g>
- Wang, L., Shen, C., Li, C., & Chen, J. (2020). Physicochemical, functional, and antioxidant properties of dietary fiber from *Rosa roxburghii* Tratt fruit modified by physical, chemical, and biological enzyme treatments. *Journal of Food Processing and Preservation*, 44(11). <https://doi.org/10.1111/jfpp.14858>

- Wang, L., Wei, T., Zheng, L., Jiang, F., Ma, W., Lu, M., & An, H. (2023). Recent advances on main active ingredients, pharmacological activities of *rosa roxburghii* and its development and utilization. *Foods*, *12*(5). <https://doi.org/10.3390/foods12051051>
- Wang, M.-S., Fan, M., Zheng, A.-R., Wei, C.-K., Liu, D.-H., Thaku, K., & Wei, Z.-J. (2023). Characterization of a fermented dairy, sour cream: Lipolysis and the release profile of flavor compounds. *Food Chemistry*, *423*, Article 136299. <https://doi.org/10.1016/j.foodchem.2023.136299>
- Wang, W., Gao, Y.-T., Wei, J.-W., Chen, Y.-F., Liu, Q.-L., & Liu, H.-M. (2021). Optimization of ultrasonic cellulase-assisted extraction and antioxidant activity of natural polyphenols from passion fruit. *Molecules*, *26*(9), 2494. <https://www.mdpi.com/1420-3049/26/9/2494>.
- Wu, H., Li, M., Yang, X., Wei, Q., Sun, L., Zhao, J., & Shang, H. (2020). Extraction optimization, physicochemical properties and antioxidant and hypoglycemic activities of polysaccharides from roxburgh rose (*Rosa roxburghii* Tratt.) leaves. *International Journal of Biological Macromolecules*, *165*, 517–529. <https://doi.org/10.1016/j.ijbiomac.2020.09.198>
- Yeo, H., Balagiannis, D. P., Koek, J. H., & Parker, J. K. (2022). Comparison of odorants in beef and chicken broth—Focus on thiazoles and thiazolines. *Molecules*, *27*.
- Zhang, R., Cao, C., Bi, J., & Li, Y. (2022). Fungal cellulases: Protein engineering and post-translational modifications. *Applied Microbiology and Biotechnology*, *106*(1), 1–24. <https://doi.org/10.1007/s00253-021-11723-y>
- Zhao, Q., Du, G., Zhao, P., Guo, A., Cao, X., Cheng, C., & Wang, X. (2023). Investigating wine astringency profiles by characterizing tannin fractions in Cabernet Sauvignon wines and model wines. *Food Chemistry*, *414*, Article 135673. <https://doi.org/10.1016/j.foodchem.2023.135673>
- Zhao, X., Tang, F., Cai, W., Peng, B., Zhang, P., & Shan, C. (2023). Effect of fermentation by lactic acid bacteria on the phenolic composition, antioxidant activity, and flavor substances of jujube–wolfberry composite juice. *LWT*, *184*. <https://doi.org/10.1016/j.lwt.2023.114884>

Further reading

- Genment, L. J. V. (2015). *Compilations of Flavour Threshold Values in Water and Other Media*. Beijing: Science Press. Second Enlarged Revised Edition.